D 2/4

DDT-A 3-DIMENSIONAL PROGRAM FOR THE ANALYSIS OF BOWED REACTOR CORES

R. MENSSEN

INTERATOM, Internationale Atomreaktorbau GmbH, –9110–, D-5060 Bergisch Gladbach 1, Germany

SUMMARY

The influence of temperature gradients, neutron fluence gradients and irradiation induced creep leads to individually different bowing effects of all elements in a core of a fast reactor. Subsequent contacts between neighbouring elements result in forces of different value. Eventually all elements will arrange in such a way, that an equilibrium of forces between all elements is achieved. The determination of this equilibrium configuration in different operational states of the reactor is of high significance especially for safety aspects.

For this reason, in addition to existing 2-dimensional codes, a 3-dimensional code was developed, to allow a good description of the whole core bowing behaviour. Each single hexagonal element is described by a simple beam with 6 springs in horizontal planes where contact with other elements is possible. Each force is divided in x- and y-directions of the coordinate system. The contact forces must be in equilibrium with the mechanical displacements in both directions. Because friction forces are not included in this analysis, all forces are assumed to act normal to contacting surfaces. Gaps may open and close and contact forces may only be compressive. Because of these nonlinearities, standard mathematical techniques for solving linear structural problems are not directly applicable. So an iterative procedure is applied to achieve the equilibrium force configuration. Each iteration step corrects the largest force discrepancy between neighbouring elements. This technique requires a long computer running time to converge, but the locations of gaps and contacts normally do not change if a rough equilibrium is found. This gap distribution is used to formulate a set of linear equations which can be solved directly. The solution is checked against the start-up gap distribution.

The code can handle 30°, 60°, 120° sectors of complete reactor cores. The system boundaries are symmetrically.

The next step of the development is to take the friction forces into consideration which originate from the different directions of element movements.

Results for a 120° sector of the KNK II reactor and for a 30°-sector of SNR 300 are available. Compared with 2-dimensional calculations the 3-dimensional calculations show following advantages:

- influence of special individual elements f.i. absorber elements is seen,
- the azimuthal distribution of radial forces on the outer support rings of the core can be obtained,
- the forces and position of elements between radial spokes are calculated,
- creep bowing is much better determined.

1. Introduction

In the core design and analysis of fast reactors, there are a number of problems related to the effects of bowing of reactor assemblies. Structural reactivity effects occur during startup, transients, and long-term usage because the ducts can bow due to temperature, creep and swelling effects. For an effective design adequate analytical methods for the prediction of these effects are required. At present, such analyses can be performed using computer programs such as NUBOW of ANL/1/ or FIAT of INTERATOM /2/. Both of them are treating the core in an two-dimensional model.

In order to describe the behaviour of all reactor assemblies in every possible situation one needs a program which is treating the core in a three-dimensional model. Such situations are earth quakes, motions during management, slip and stick effects, accidental conditions, tolerances of the load-pad clearances and others.

Especially a heterogeneous core can be calculated satisfactorily with a three-dimensional model only. For all these reasons a three-dimensional code named DDT has been developed, allowing a good description of the whole core bowing behaviour. In the following chapters some important features of the program are discussed in detail.

2. Mechanical Model of the Ducts

To reduce computer time a simple model is used for the ducts, with the option to include a more sophisticated model later on. Each single hexagonal element is considered to be an elastic beam with local flexibility, represented by six springs in each plane where contact between adjacent elements is possible (Fig. 1). The program evaluates the effects of beam bending due to contact forces by means of unconstrained-beam stiffness matrices. These matrices B_{jk} are set up for each beam using conventional beam theory /1/. Deflections due to forces are described as mechanical deflections V_{ijk}.

The unconstrained bow shapes are calculated using conventional beam theory, assuming each beam is subjected to an equivalent bending moment /1/ /2/ and the deflections of the x- and y-directions are independent from each other. The thermal, swelling and creep bow shapes are added up forming the unrestrained bow shape VB_{ijk}.

The effect of local flexibility at contact points is included. It is assumed that the load pads can be represented by independent mechanical springs connected to the beam centreline. This representation is shown in fig. 2 for the adjacent beams j-1 to j+1. Because a load pad is formed by a continous hexagonal ring, a normal force acting on one face of a load pad causes local deflections of all six faces. This complexity is not included in the analysis. Because friction forces are not yet included in the analysis, all forces are assumed to act normal to contacting surfaces. Summarizing, the same well known models are used as in the two-dimensional codes.

3. Coordinate System

As the elements are hexagonal, it is very convenient to use a coordinate system in which the x- and y-axis form a 120° angle. The x-y plane is located in the support plane and the z-axis is vertical to it, as shown in fig. 3.

So all forces and deflections are described in the x-z and y-z plane. How the elements are placed relative to the x- and y-axis is shown in fig. 4. The third axis of a hexagon is called s-axis. A contact force acting in this direction has to be divided into the x- and y-direction of the coordinate system.

$$Px = Px + Ps \qquad Py = Py + Ps \qquad (1)$$

The deflections are defined relative to a local z-axis, the unbowed centreline of each element.

4. Contact and Bending Forces

If the sum of the deflections V + VB is larger than the gap, Dx is the clearance between adjacent elements, contact will occur and the contact force is

$$P_{ij} = (V_{ij} + VB_{ij} - V_{ij+1} - DX_{ij})\, K^{+}_{ij} \qquad (2)$$

where K^{+} is the series combination of the two contacting springs. Eq.(2) is nonlinear and applies only if contact is made; otherwise, the force P_{ij} would be zero. This nonlinearity is treated in our program DDT by testing the algebraic sign of the expression in brackets and setting K_{ij} to zero if it is negative. Eq.(2) is only two-dimensional, as the contact forces are not independent of the displacements in the other direction of the coordinate system due to the 120° angle between the axis, the contact forces are

$$Px_{ijk} = Kx_{ijk} \{ [Vx+VBx-(Vy+VBy)/2]_{ijk} - [Vx+VBx-(Vy+VBy)/2]_{ij+1k} - Dx_{ijk} \}$$

$$Py_{ijk} = Ky_{ijk} \{ [Vy+VBy-(Vx+VBx)/2]_{ijk} - [Vy+VBy-(Vx+VBx)/2]_{ijk+1} - Dy_{ijk} \} \quad (3)$$

$$Ps_{ijk} = Ks_{ijk}/2 \{ [Vx+VBx+Vy+VBy]_{ijk} - [Vx+VBx+Vy+VBy]_{ij+1k+1} - Ds_{ijk} \}$$

This gives the contact forces acting on all load pads. The displacements are zero, if the subscripts j+1 or k+1 are larger than the number of elements in these directions, or are to be determed by the system bounderies conditions, which are symmetrical.
The forces acting on all fixed supports are

$$Px_{ijk} = Kx_{ijk} [Vx + VBx - (Vy + VBy)/2]_{ijk}$$

$$Py_{ijk} = Ky_{ijk} [Vy + VBy - (Vx + VBx)/2]_{ijk} \quad (4)$$

$$Ps_{ijk} = Ks_{ijk}/2 [Vx + VBx + Vy + VBy]_{ijk}$$

Because of no importance for our considerations, clearances are not taken into consideration at the supports, but it is possible, too.
The bending forces are

$$Bx_{ijk} = \sum_{h=1}^{n} a_{hijk} Vx_{hjk}$$

$$(5)$$

$$By_{ijk} = \sum_{h=1}^{n} a_{hijk} Vy_{hjk}$$

where a_{hijk} are the beam-stiffness coefficients of the element jk and n is the number of load planes. It is assumed that the bending forces are independent of deflections in the other direction. The contact forces have to be in an equilibrium with the bending forces.

$$Px_{ijk} - Px_{ij-1k} + Ps_{ijk} - Ps_{ij-1k-1} = Bx_{ijk}$$

$$(6)$$

$$Py_{ijk} - Py_{ijk-1} + Ps_{ijk} - Ps_{ij-1k-1} = By_{ijk}$$

5. <u>Direct Solution</u>

If the gap distribution is known, which normally is not the case, eq.(3) to eq.(6) are representing a set of linear equations, which can be solved directly. These equations can be written as a matrix equation (7)

$$P = S \cdot V \quad (7)$$

V is a matrix with the unknown mechanical displacements of each element at the load pads and supports in the x- and y-directions. S is a stiffness matrix of the elements in the considered core section. P is a matrix with the forces at the load pads and supports due to thermal, swelling and creep bowing and the clearances between the elements.
Eq.(7) is solved with well known techniques like Gaus-Seidel. To save computertime and place, the special structure of the matrix S is used.

6. Iteration technique

In addition to the direct solution, an iteration technique has to be used, because the unknown gap distribution represents a nonlinearity of the linear eq.(7).
At first, a point-relaxation process was developed. It solved eq.(6) by correcting the largest force discrepancy. But the computer running time for small problems was extremely large. Therefore, other techniques were looked for. Eventually, the following procedure was found:

Starting with an arbitrary gap distribution by assuming the mechanical deflections V_{ijk} to be zero, eq. (7) is solved. The resulting mechanical deflections V_{ijk} lead to a new gap distribution, which is fed again into eq. (7). This procedure has to be repeated only a few times till the gap distribution has converged, which is achieved in relatively short running time. This final distribution is tested by checking the force equilibrium for each single element (eq. (6)). According to all our experience, the obtained gap distribution is correct and therefore the mechanical displacements are the solution leading to a minimum of stored elastic energy.

This gap iteration technique has been installed in the FIAT-program /2/ which allowed a direct comparison with the blockrelaxation process of NUBOW /1/. As a result, considerable computer-time savings of roughly a factor of ten can be gained with the gap iteration technique.

7. The Program DDT

The program was written to calculate the equilibrium forces and displacements of a series of beams with clearances and flexibilities at contact points, when subjected to an imposed set of temperature gradients. For this purpose the gap iteration technique is applied, in which the gap distribution is assumed, to solve linear equations.

The program is tested for a 30° sector with 12 rows of elements and a 120° sector with 6 rows of elements. For comparisons sake the program can calculate radial spokes like FIAT.

It is possible to use different duct diameters in the x,y,z-direction to hand fabrication tolerances.

The program can modify the temperature bowing shapes in steps to calculate different power levels. In principle, it is possible to simulate bowing due to swelling by altering the temperature bowing shapes.

Two different geometries of core restraint systems can be taken into account, which are shown in fig.5 and 11.

The output of the program is done by a plot routine, which shows the contact forces (in Newtons) between adjacent elements, the deflections due to temperature gradients (thin lines) and the deflections due to forces (thick lines). At the upper load plane the equilibrium positions are marked with a cross. At the lower load plane there are no temperature gradients and therefore no temperature deflections.

The next steps of development will include:

- swelling and creep due to neutron fluence
- different management schemes for the assemblies
- friction forces

8. Two applications

a) 30^{o} sector with 42 elements

Figures 5 and 6 are showing the upper and lower load plane of a 30^{o}sector and in addition the figures contain the results of a spoke calculation. It can be seen how bridging forces are changing the equilibrium condition in this case. Therefore a direct comparison is possible between a three- and a two-dimensional calculation.

Figures 7 and 8 are showing a sector with different duct diameters as in figures 5 and 6. In both cases the wall thickness is 2.6/mm/ and the duct diamters of each element are arbitrarily chosen having a value between 114.98/mm/ and 115.05/mm/. This leads to different distributions of clearances between the elements in both cases.

Figures 9 and 10 are showing a sector with elements which have temperature gradients two times larger as before, therefore the forces are much higher.

b) 120^{o} sector with 36 elements

Figures 11 and 12 are showing the upper and lower load plane of a 120^{o} sector. Though the outermost elements are drawn as hexagons, the calculation was performed with cylindrical elements and a straight restrain plane on the upper load plane, so that the contact occurs at one point only. The contact forces are divided into the x- and s- or y- and s-direction. The arbitrary duct diameters were chosen between 128.98/mm/ and 129.05/mm/ and the wall thickness is 2.6/mm/.

For all shown applications the calculation time was about one minute on a CD 6500 computer.

References

/1/ McLENNAN, G.A., " A FORTRAN-IV Program for the Static Elastic Structural Analysis of Bowed Reactor Cores," ANL-8068, April 1974

/2/ URBAN, K., " Analysis of Bowed Reactor Cores Using the FIAT-Program," 4th SMIRT-Conference San Francisco 1977

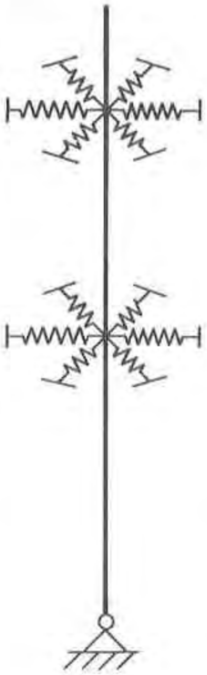

Fig.1 Mechanical model of a reactor assembly

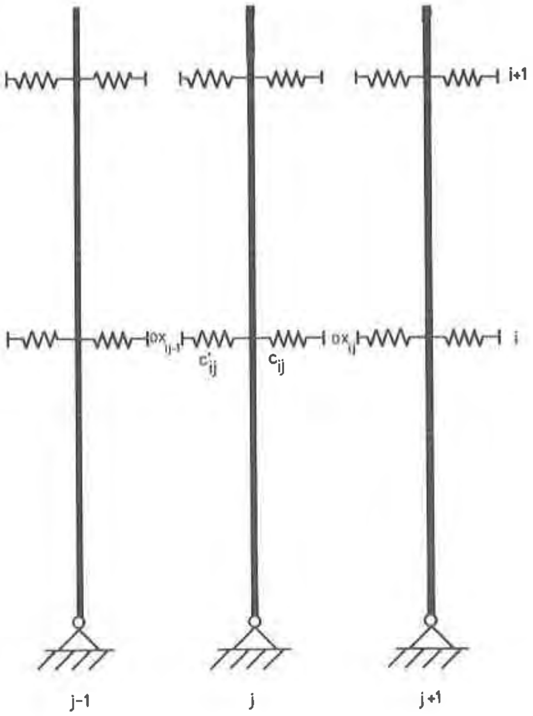

Fig.2 Elements in a row k with clearance and load pad stiffness

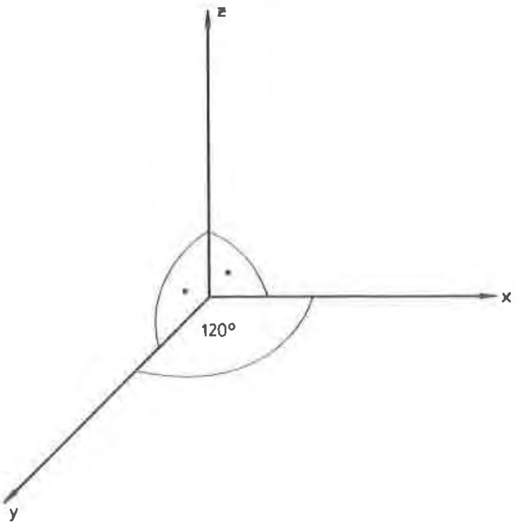

Fig.3 Coordinate system

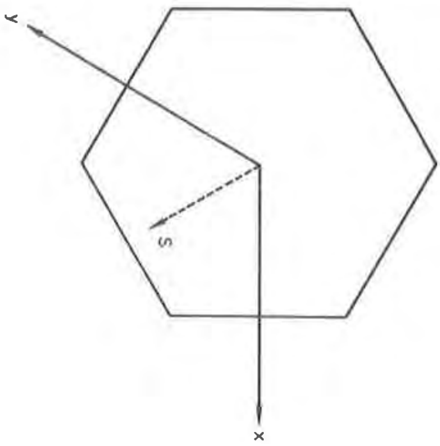

Fig.4 Position of an assembly cross-section in a x-y plane

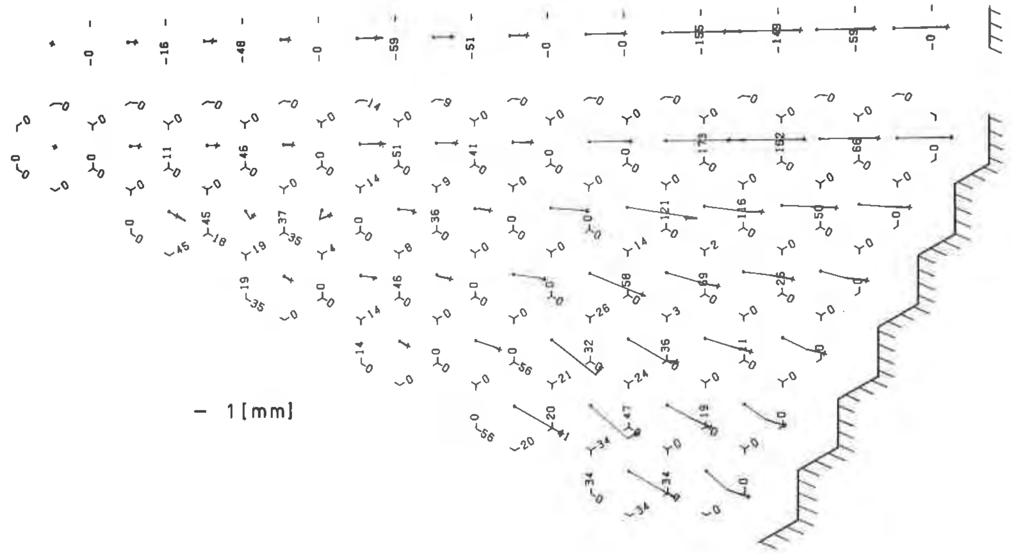

Fig.6 Lower load plane, 30° sector

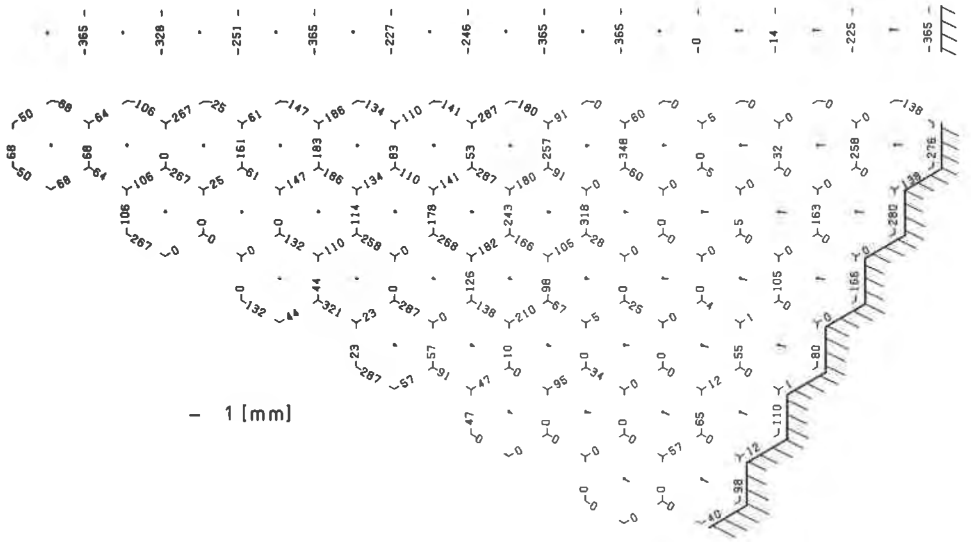

Fig.5 Upper load plane, 30° sector

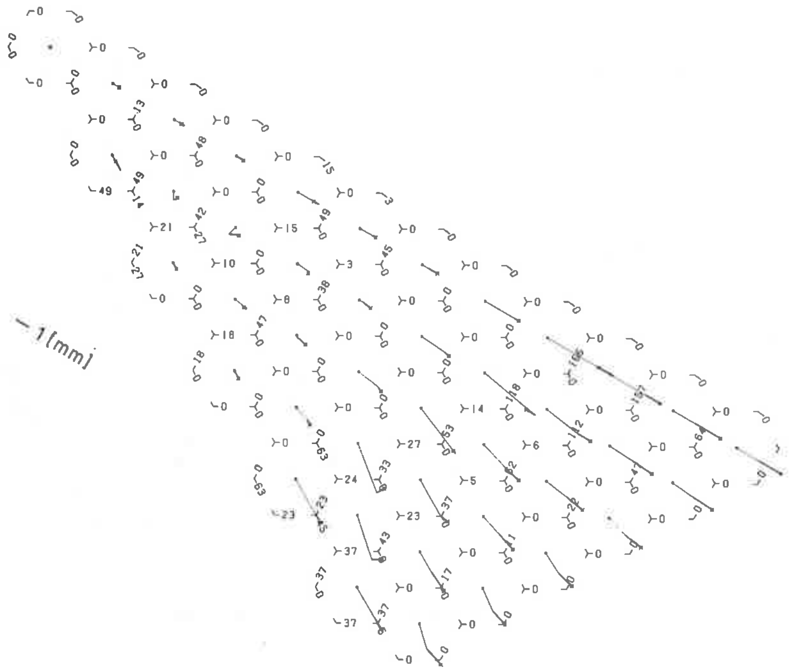

Fig.7 Upper load plane, 30° sector, clearance distribution changed

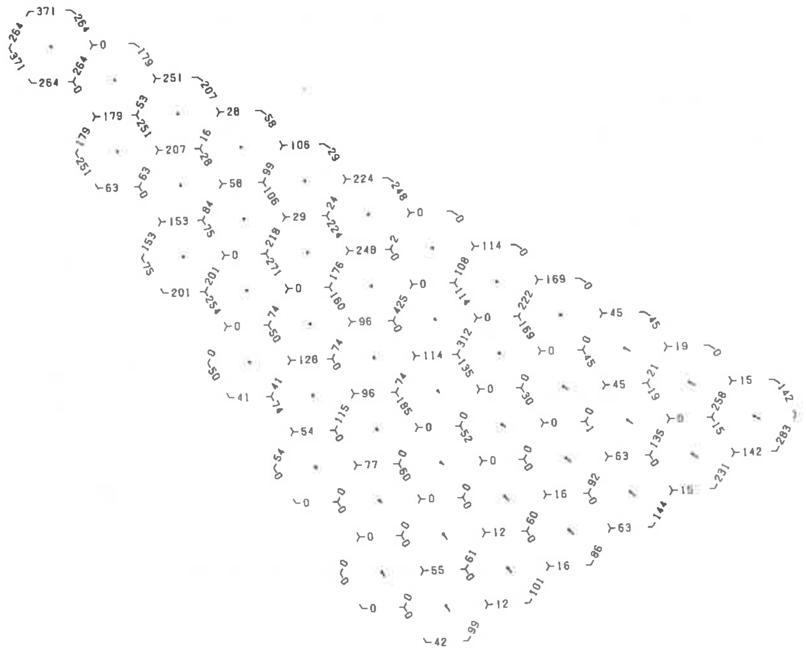

Fig.8 Lower load plane, 30° sector, clearance distribution changed

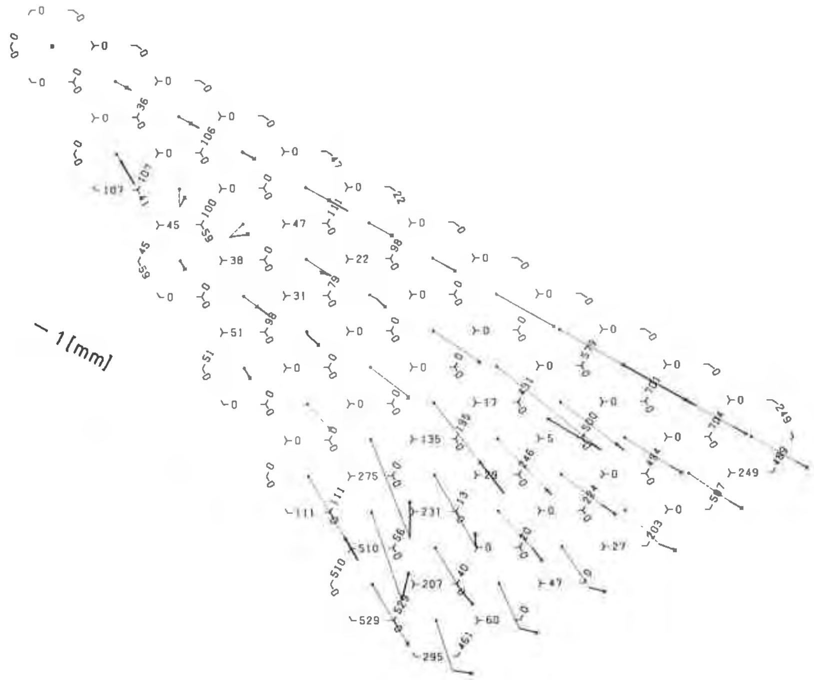

Fig.9 Upper load plane, 30° sector, double temperature gradients

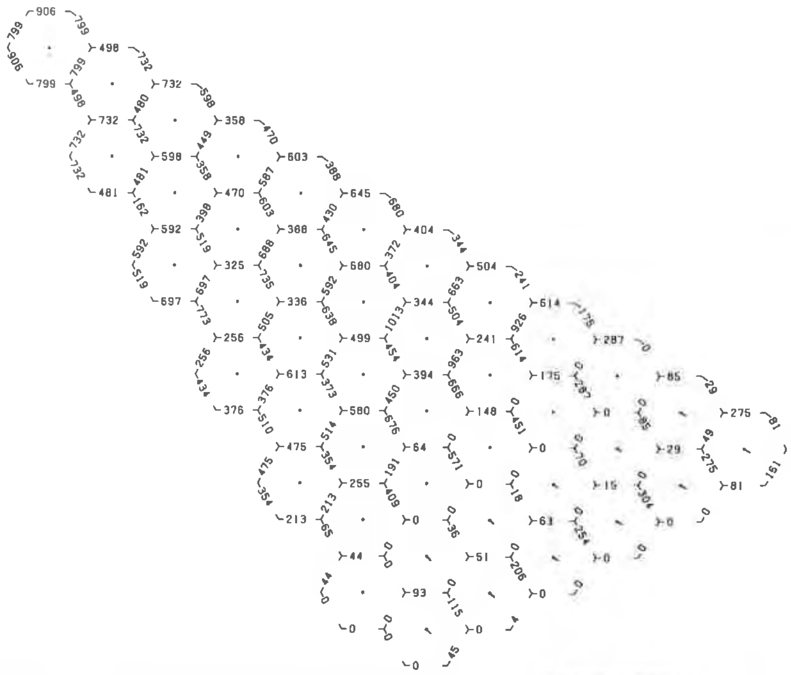

Fig.10 Lower load plane, 30° sector, double temperature gradients

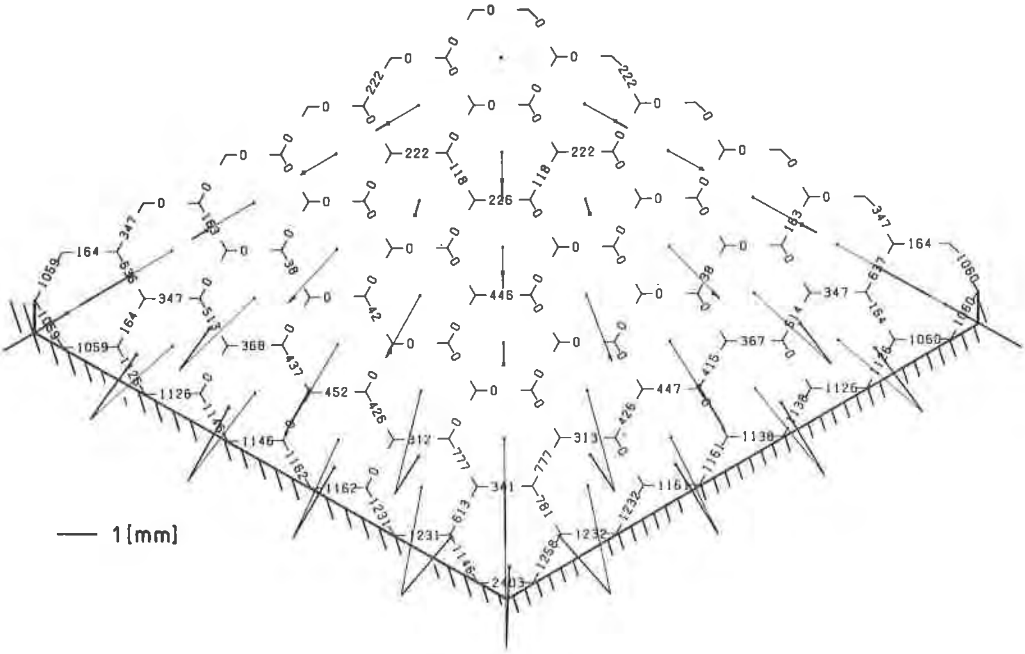

Fig.11 Upper load plane, 120° sector

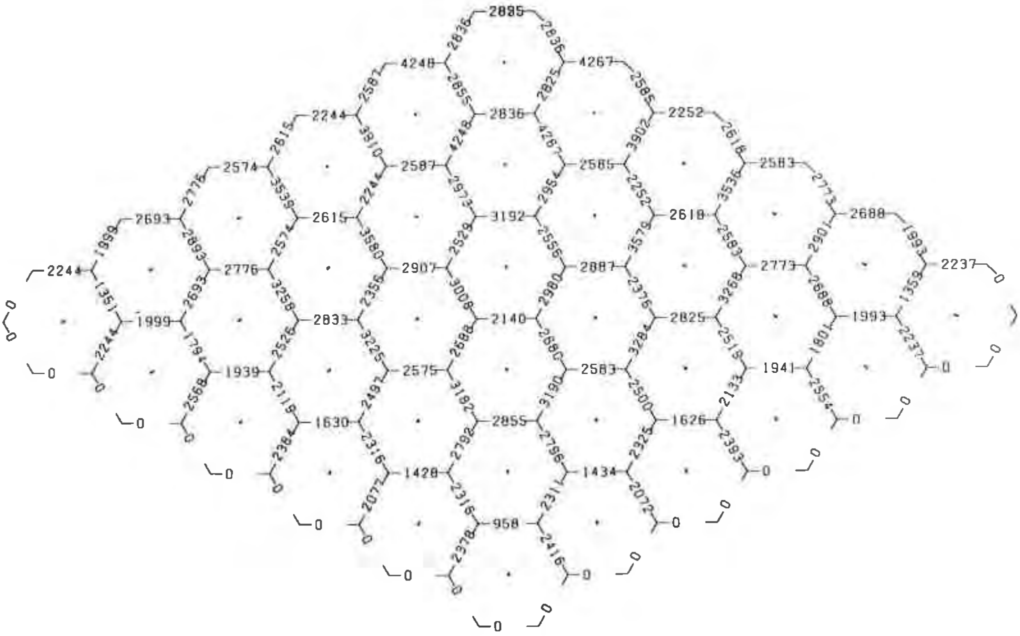

Fig.12 Lower load plane, 120° sector